



Eur. Phys. J. E (2019) **42**: 137

DOI 10.1140/epje/i2019-11907-7

Elucidating the impact of extreme nanoscale confinement on segmental and chain dynamics of unentangled poly(cis-1,4-isoprene)

Thomas Kinsey, Emmanuel Mapesa, Tyler Cosby, Youjun He, Kunlun Hong, Yangyang Wang, Ciprian Iacob and Joshua Sangoro







Regular Article

Elucidating the impact of extreme nanoscale confinement on segmental and chain dynamics of unentangled poly(cis-1,4-isoprene)***

Thomas Kinsey¹, Emmanuel Mapesa¹, Tyler Cosby¹, Youjun He², Kunlun Hong², Yangyang Wang², Ciprian Iacob^{3,4}, and Joshua Sangoro^{1,a}

- Department of Chemical and Biomolecular Engineering, University of Tennessee, Knoxville, TN 37996, USA
- ² Center for Nanophase Materials Science, Oak Ridge National Laboratory, Oak Ridge, TN 37831, USA
- ³ National Research and Development Institute for Cryogenic and Isotopic Technologies, ICSI Rm. Valcea, Rm. Valcea, Romania
- ⁴ Karlsruhe Institute of Technology (KIT), Institute for Chemical Technology and Polymer Chemistry, 76128, Karlsruhe, Germany

Received 5 July 2019 and Received in final form 30 August 2019 Published online: 25 October 2019

© EDP Sciences / Società Italiana di Fisica / Springer-Verlag GmbH Germany, part of Springer Nature,

Abstract. Broadband dielectric spectroscopy is employed to probe dynamics in low molecular weight poly(cis-1,4-isoprene) (PI) confined in unidirectional silica nanopores with mean pore diameter, D, of 6.5 nm. Three molecular weights of PI (3, 7 and $10\,\mathrm{kg/mol}$) were chosen such that the ratio of D to the polymer radius of gyration, R_g , is varied from 3.4, 2.3 to 1.9, respectively. It is found that the mean segmental relaxation rate remains bulk-like but an additional process arises at lower frequencies with increasing molecular weight (decreasing D/R_g). In contrast, the mean relaxation rates of the end-to-end dipole vector corresponding to chain dynamics are found to be slightly slower than that in the bulk for the systems approaching $D/R_g \sim 2$, but faster than the bulk for the polymer with the largest molecular weight. The analysis of the spectral shapes of the chain relaxation suggests that the resulting dynamics of the $10\,\mathrm{kg/mol}$ PI confined at length-scales close to that of the R_g are due to non-ideal chain conformations under confinement decreasing the chain relaxation times. The understanding of these faster chain dynamics of polymers under extreme geometrical confinement is necessary in designing nanodevices that contain polymeric materials within substrates approaching the molecular scale.

1 Introduction

The design of nanostructured polymer-based devices—such as photoresists, batteries, sensors for smart drug delivery, organic electronics gadgets etc.— requires a detailed understanding of the interplay between decreasing product size, geometrical restriction, and polymer dynamics. Mechanisms associated with local polymer dynamics such as chain interpenetration, adsorption, configuration and conformation, all of which determine macroscopic material properties, are known to be influenced by spatial confinement [1–6]. For example, conformations of polymer chains in the bulk phase can

https://doi.org/10.1140/epje/i2019-11907-7

be quantitatively described in terms of the radius of gyration (R_q) . However, in the vicinity of solid surfaces, the conformations of the polymer chains are altered in a myriad of ways affecting the stiffness of the chain, free space for random motion of segments, etc., due to the nature of the interactions with the solid surface and the time-scales of these interactions. These interactions lead to changes in polymer dynamics and resultant physical properties compared to the corresponding bulk system [7– 10]. For the case of confined polymers in nanoporous media, the length- and time-scales of these interactions can be investigated by varying the diameter of the pores and/or increasing the size (molecular weight) of the macromolecules. Some of the polymers whose dynamics have been investigated under confinement in nanopores include poly(2-vinylpyridine) [11], poly(dimethyl siloxane) (PDMS) [12,13], poly(methylphenyl siloxane) [12, 14,15], poly(ethylene-alt-propylene) [16], poly(ethylene

 $^{^\}star$ Contribution to the Topical Issue "Dielectric Spectroscopy Applied to Soft Matter" edited by Simone Napolitano.

 $^{^{\}star\star}$ Supplementary material in the form of a .pdf file available from the Journal web page at

a e-mail: jsangoro@utk.edu

glycol) [17], poly(propylene glycol) (PPG) [6,13,18-22], and poly(cis-1,4-isoprene) (PI) [23-25].

A particular subset of dielectrically active Type-A polymers [26] (such as PPG and PI) present an ideal model to study the segmental and chain dynamics due to the non-zero components of the segmental dipole moment perpendicular and parallel to the chain contours, respectively. Thus, two dielectrically active relaxations at completely different time-scales can be studied by broadband dielectric spectroscopy (BDS). For these systems, BDS provides insight into the effect of confinement on both local and global dynamics which are critical for determining polymeric properties such as the glass transition and viscoelasticity, all of which are altered when the polymer is placed under confinement.

The majority of investigations of confined polymers have focused on thin films deposited on inorganic substrates for confinement in one dimension or infiltrated into nanoporous media for two-dimensional confinement. Previous studies of the Type-A PI in nanopores have employed either controlled porous glass (CPG) [23] or anodized aluminum oxide (AAO) membranes [24,25]. The latter system has the advantage of a narrow distribution of pore diameters. However, the chemistry of these membranes limits the smallest obtainable pore diameter to about 20 nm, and restricts the extent of possible confinement to that of several molecules [27]. In their study of PI confined in CPG, Petychakis et al. [23] showed that, depending on the size of the chain relative to pore radius, the normal mode was broadened due to topological constraints imposed on the chain. In a similar work, using self-ordered AAO pores, Alexandris et al. [24] demonstrated that a broadened distribution of relaxation times for the PI chain motion occurs even for pore sizes that are 50 times larger than the unperturbed chain dimensions, and argued that at such (low) levels of confinement, chain adsorption plays a more significant role than confinement itself. Related studies, such as the neutron spin echo study of PDMS by Krutyeva et al. or the pulsed field gradient NMR study of PPG by Schönhals et al., suggest that a two-layer model consisting of an adsorbed layer at the pore wall and a bulk layer is oversimplified and suggest a dynamical or interphase layer where time-scales of the interactions of adsorbed and bulklike chains cause a gradual slowing in the molecular motions of chains within the nanopores compared to bulk [5, 6]. Generally, these studies observed changes in the dynamics due to surface interactions, but the length-scales of the confinement rarely approached that of the R_g of the confined polymer chain. Therefore, the extent of the effect of geometrical confinement on the underlying relaxation dynamics of polymer segments and chains remains unresolved.

In the present work, we infiltrate unidirectional silica pores with mean diameter (D) of 6.5 nm with PI and systematically vary the molecular weight of the polymer so that, for the longest chains studied, $D/R_g \approx 1.9$. To this end, the aim is to increase the extent of confinement such that no bulk like layer presumably exists, and a high probability that all polymer chains interact with the pore surface, or at least some interphase layer where the molecules

"feel" the effects of the confined chains, is achieved. To the best of our knowledge, this level of confinement for PI has not been previously reported. These results show changes in the spectral shapes and time-scales of the chain relaxation when the radius of gyration (R_g) of the polymer becomes comparable to the length-scale of the nanopore. We show that drastic changes to the chain dynamics occur at these extreme levels of confinement, and attribute these changes to the non-ideal conformations that the polymer chains are forced to assume because of geometrical constraints.

2 Materials and methods

Three cis-1,4-polyisoprene (PI) polymers ($M_n=3.5$ (PDI = 1.05), $M_n=7.4$ (PDI = 1.08), and $M_n=10.3$ $(PDI = 1.09) \, \text{kg/mol}$, termed 3 k, 7 k and 10 k, respectively) having narrow molecular weight distributions were synthesized using anionic polymerization techniques under high-vacuum conditions (10^{-6} mmHg) in a glass apparatus equipped with break-seals. All reagents were purified according to reported procedures [28]. The polymerization was carried out in benzene at 25 °C and sec-butyllithium was employed as the initiator and degassed methanol was used as the terminator. The material was precipitated in non-solvent and washed several times. The resulting polymer was characterized by size exclusion chromatography (SEC) equipped with refractive index and light scattering detectors. ¹H NMR and ¹³C NMR spectra were used to confirm the microstructures of the PIs. Dielectric experiments were performed on a Novocontrol High-Resolution Alpha Analyzer equipped with a Quatro system with the capability of controlling temperature to a precision of 0.1 K under dry nitrogen atmosphere. Bulk dielectric measurements were made by applying 1.5 V across a parallel plate capacitor prepared by sandwiching the polymer between two 15 mm diameter brass electrodes with two $100 \,\mu\mathrm{m}$ silica rod spacers to maintain sample thickness. The frequencies of the applied alternating electric field and temperatures ranged from 10^{-1} – 10^{7} Hz and 200– $320\,\mathrm{K}$ at 5 K intervals, respectively. The same applied potential, frequency range and temperatures employed for bulk systems were used for dielectric measurements of PI in pores.

The silica nanopores were prepared by wet electrochemical etching of a highly doped $\langle 100 \rangle$ oriented silicon wafer in a home-built set-up. The resulting silicon pores were washed several times with reverse osmosis milliQ water, then oxidized by heating in a furnace at 700 °C for 5 hours, then 880 °C for 6 hours. Under these preparatory conditions, previous characterization work using NMR-cryoporometry and scanning electron microscopy (SEM) shows that unidirectional, 6.5 nm diameter porous silica membranes with a porosity of 7% are obtained [21–23]. The membranes were dried to remove any excess adsorbed moisture by heating to 250 °C under 10^{-8} mbar oil-free vacuum for 24 hours before infiltrating the polymers.

Polymers were infiltrated into nanoporous silica membranes by coating both surfaces of the membrane then pulling a 10^{-8} mbar vacuum and heating to 60 °C for

40–48 hours. Then, immediately upon cooling to room temperature and removal from the vacuum, excess material on the surface of the pores was removed using Kimwipes and lens paper, then subsequently sheared multiple times between clean glass slides until no residual polymer was transferred from the membranes to the slides. Then the parallel plate capacitor was prepared for dielectric measurements by placing 6 mm diameter, 750 nm thick aluminum foil disks concentrically to each side of the membrane to ensure proper electrical contact with the two 6 mm brass electrodes. The confined polymer was then immediately measured over the temperature range above. This filling and measurement procedure was rigorously followed to ensure the equilibration dynamics (that have been reported to occur at much longer time-scales than that of the polymer chain dynamics and viscoelastic flow) for each of the different PI samples under confinement are held constant throughout this study [29]. In that way, only the effects of the polymer confinement on chain dynamics as a function of the M_w of the PI are probed. By maintaining a constant pore diameter, the relative amount of polymer segments in contact with the pore surface is constant across each sample, and thus the kinetics of surface adsorption and equilibrium dynamics are not considered [30]. We did consider, however, the possibility of air pockets being trapped in the PI after infiltration into the pores. This possibility is discussed in the Electronic Supplementary Material (ESM, figs. S1 and S2) in terms of Maxwell-Wagner-Sillars polarization theory and experimental evidence that air inclusions, if any exists, have negligible impact on the main results reported in this article.

3 Results & discussion

The dielectric loss (ε'') corresponds to energy from the electric field lost by dipolar relaxation. The ε'' spectra for all polymers in bulk and under confinement are displayed in fig. 1 at selected temperatures. The spectra for bulk PI are displayed in open symbols and show two distinct dielectric relaxations. First, a higher-frequency process is observed at lower temperatures, and corresponds to the segmental relaxations [31]. The spectral shape corresponding to the segmental relaxation is not altered under confinement; however, the rates of maximum loss for this relaxation peak are faster at corresponding temperatures. Second, a slower relaxation in bulk corresponding to the end-to-end dipole vector of the chain is observed at higher temperatures. This relaxation decreases in rate with increasing molecular weight [32]. In contrast to the modest effect of confinement on the segmental relaxation, the chain dynamics are significantly altered for each polymer within the 6.5 nm pores. This polymer is known to have a higher-frequency β relaxation wing attributed to libration motions at local length-scales which is observed in bulk at the lowest temperatures [33]. These β relaxations are too weak to be observed under confinement and are therefore not investigated further.

A significantly broad relaxation dominates the spectra at intermediate time-scales for all polymers within 6.5 nm

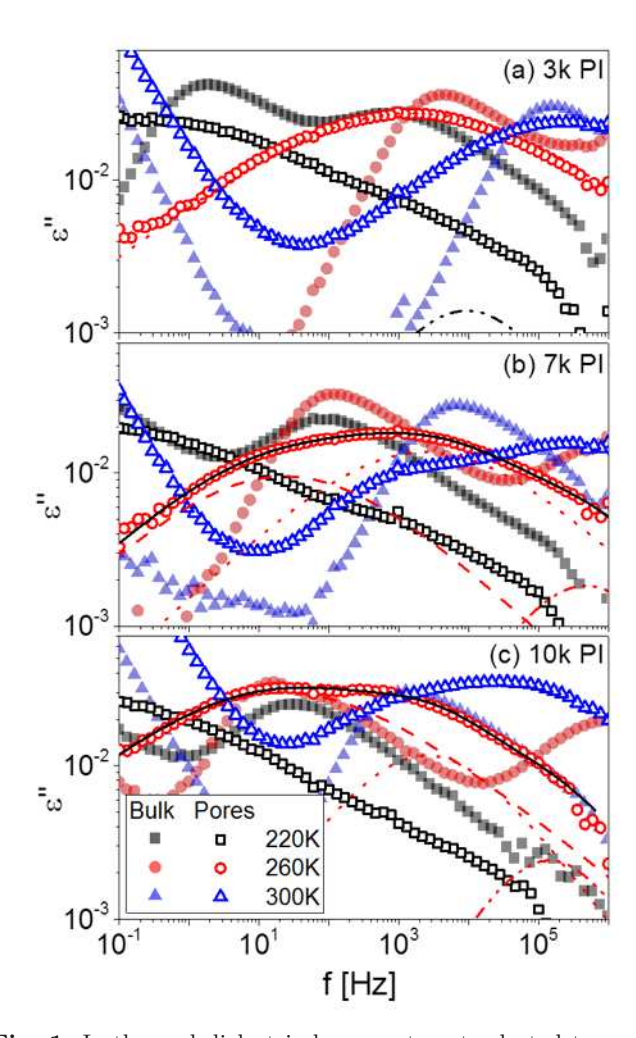


Fig. 1. Isothermal dielectric loss spectra at selected temperatures for the $3\,\mathrm{k}$ (a), $7\,\mathrm{k}$ (b) and $10\,\mathrm{k}$ (c) polymers in bulk (closed symbols) and in pores (open symbols). Fit lines from eq. (1) are included for the segmental relaxation (dash-dotted), CCR (dotted) and slow mode (dashed) at 260 K, as well as a linear combination of all fits (solid lines). The segmental relaxation is outside the measurement window for the $3\,\mathrm{k}$ PI in pores, therefore, the fit for this relaxation is shown for 220 K instead.

pores (see dotted fit lines in fig. 1), with the segmental relaxation only observed as a high-frequency wing at low temperatures (see dash-dotted fit lines in fig. 1). At high temperatures, a low-frequency shoulder is observed emerging from this dominant, intermediate relaxation. This low-frequency shoulder is barely visible for the confined 3 k PI and becomes more prominent with increasing molecular weight (see dashed fit lines is fig. 1). To be consistent with previous reports in the literature of confinement-induced relaxations, we will term the intermediate relaxation the confined chain relaxation, or CCR [34]. The shape of this CCR is well described by the empirical Cole-Cole function (eq. (1)) for the 3 k PI. The Cole-Cole function for the dielectric loss is given by

$$\varepsilon^* - \varepsilon_\infty = \frac{\Delta \varepsilon}{(1 + (i\omega\tau)^\alpha)}, \qquad (1)$$

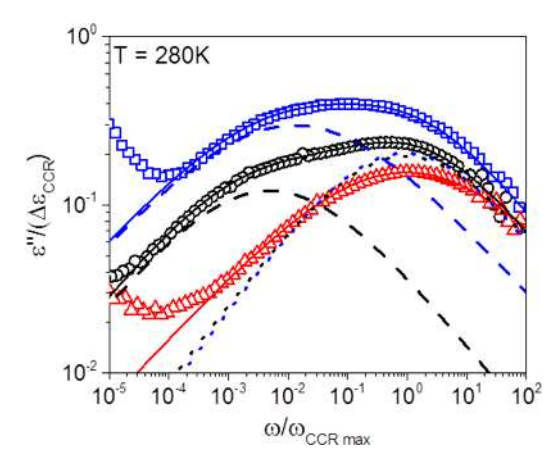


Fig. 2. Dielectric loss normalized by the dielectric relaxation strength and mean relaxation rate of the CCR for 3 k (triangles), 7 k (circles) and 10 k (squares) within 6.5 nm pores. The fit lines from eq. (1) are shown for the CCR (dotted) and the slow mode (dashed) and the summation of all fits (solid). The 3 k PI, having no fit for the slow mode only displays the CCR relaxation fit (red solid line).

where ε^* is the complex dielectric function, ε_{∞} is the highfrequency limit of the real part of ε^* , $\Delta \varepsilon$ is the dielectric relaxation strength, ω is the angular frequency of the applied field, τ is the relaxation time, and α is the shape parameter. For the 7k and 10k PI a linear combination of two Cole-Cole functions is required for the additional low-frequency process that emerges with increasing molecular weight. We will term this low-frequency process the slow chain mode or slow relaxation. The mean rates of the maximum loss for these Cole-Cole fits are displayed in fig. 4 and will be discussed later. A possible consideration of this low-frequency process that emerges with increasing M_w of PI under confinement is that a recently described chromatographic phenomena of M_w occurs during imbibition of polymers into pores [35]. It was observed that the capillary filling of smaller polymer chains into pores occurs faster than larger ones. If this were the case, we may expect a skewed distribution of PI chain relaxations toward low frequencies. However, the bimodal distribution of the PI chain relaxations (we term the CCR and slow mode) is not explained by this phenomena. Additionally, the extremely low PDIs of the PI in this study exclude overlap of molecular weights present in each of the samples used in this study. Therefore, this slow mode is due to effects of confinement on the polymers of various molecular weights in the 6.5 nm pores, and is not chromatographic in nature.

Figure 2 displays the dielectric loss spectra at $T=280\,\mathrm{K}$ normalized by the average rate $(\omega_{CCR\,max})$ and dielectric strength of the CCR Cole-Cole fit $(\Delta\varepsilon_{CCR})$. A low-frequency shoulder clearly emerges with increasing molecular weight. This slow relaxation is possibly present for the confined 3 k PI, but it is too weak to be accurately fit along with the CCR. The shape parameter, α , in the Cole-Cole fit function (see eq. (1)) for the CCR increases slightly with increasing molecular weight and decreases with decreasing temperature (see fig. 3(a)). A decrease in α indicates a symmetric broadening in the distribution

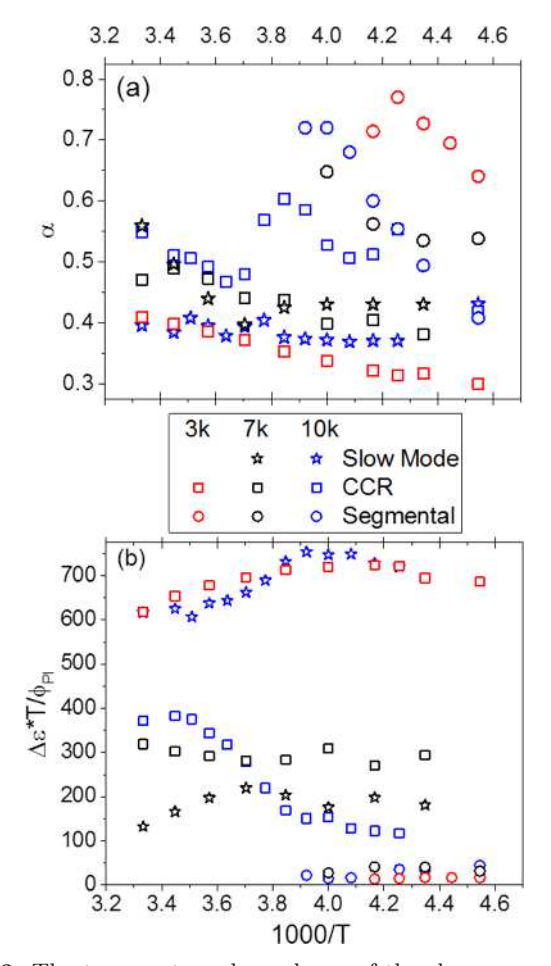


Fig. 3. The temperature dependence of the shape parameter α (a), corresponding to symmetric broadening for the Cole-Cole fits to the segmental relaxation (circles), CCR (squares) and slow modes (stars) for confined 3 k (red), 7 k (black) and 10 k (blue) PI. The dielectric strength, $\Delta \varepsilon$, normalized by temperature and volume fraction of PI (ϕ_{PI}) from eq. (2) is also displayed (b) having the same symbols and colors as fig. 3(a).

of relaxation times. Therefore, with increasing molecular weight there is an increasingly broadened distribution of relaxation times for the chains or portions of chains contributing to this CCR process and a narrowing of relaxation time distribution of the CCR with decreasing temperature for all molecular weights.

A careful analysis of the dielectric relaxation strengths, $\Delta \varepsilon$, for each relaxation fit by eq. (1) reveals unique and unexpected effects of confinement on the dynamics of the chain. The $\Delta \varepsilon$ values for all processes are normalized by temperature and PI volume fraction (ϕ_{PI}) as estimated using a 7% porosity of the silica pores (see fig. 3(b)). The dielectric relaxation strength of the chain relaxation is given by

$$\Delta \varepsilon = \frac{4\pi N_a \mu^2 \phi_{PI}}{3k_B TM} F \left\langle R^2 \right\rangle, \tag{2}$$

where n is the average number density of dipoles, μ is the dipole moment, ϕ_{PI} is the volume fraction of dipoles contributing to the relaxation, $\langle R^2 \rangle$ is the chain dipole end-to-

end distance, M is molecular weight, k_B is the Boltzmann constant, and T is absolute temperature. This normalization by ϕ_{PI} and temperature reveals segmental relaxation $\Delta \varepsilon$ values for the confined polymers that are equal to those observed in the bulk for all molecular weights (see fig. S3 in the ESM for bulk $\Delta \varepsilon$). A similar segmental relaxation strength, $\Delta \varepsilon$, in bulk and normalized segmental relaxation under confinement corresponds to a constant average number density (n) of PI segments in each measurement. The fact that these normalized $\Delta \varepsilon$ values under confinement are comparable to the bulk systems suggests that the average number density of PI segments measured are similar under confinement as they are in bulk, and also indicates the pores are completely filled with PI. The normalized $\Delta \varepsilon$ for the CCR is observed to be inversely proportional to molecular weight at low temperatures. For confined 7 k and 3 k PI, these values are relatively temperature independent, as are the strengths of the chain relaxations for all systems in bulk (see fig. S3 in the ESM). For the 10 k PI in pores, however, this $\Delta \varepsilon$ decreases with decreasing temperature. This temperature dependence of the normalized 10 k PI $\Delta \varepsilon_{CCR}$ suggests that the end-toend distance of the 10 k PI is decreasing with decreasing temperature. This is further explained through analysis of the 10 k PI slow chain mode.

The normalized $\Delta \varepsilon$ of the slow chain mode (not obvious for the confined 3k PI) for the confined 10k PI is 2-4 times higher than that measured for the 7 k PI. This increase suggests an increase in the average end-to-end distance of the 10 k PI chain under nanoscale confinement compared the 7k causing the chain to take on more nonideal conformations within the pores. This non-ideal conformation under confinement presumably results in a portion of the dipole moments in the chain to be oriented by the spatial confinement leading to this slow mode for the 7 k and 10 k PI. The spectral shape of this slow relaxation is slightly broadened for the 10 k PI compared to the 7 k, and both shapes are temperature independent. The total normalized dielectric strength (summation of $\Delta \varepsilon$ for the CCR and slow mode for the 7 k and 10 k, and $\Delta \varepsilon_{CCR}$ only for 3k) for the confined 7k and 3k PI is determined to be roughly one order of magnitude higher compared to the strength of the chain relaxation of all systems in the bulk (see fig. S4 in the ESM). This suggests that the sum of these two processes in the 7k encompasses the same relative number of chain segments contributing to the endto-end dipoles measured as for the 3 k under confinement. However, for the 10 k, in addition to the changes in the temperature dependence of the $\Delta \varepsilon$, the total normalized dielectric strength of the CCR and slow relaxations together is roughly twice that compared to the 3k and 7k PI. We suggest that this also reflects an increase in the change of $\langle R^2 \rangle$ relative to M when the molecular weight is increased to 10 k. This is supported by evidence from simulations that during polymer translocation through a nanopore, if the size of the chain is large compared to the pore size, the polymer maintains an extended conformation during translocation, while smaller chains are able to reform their bulk-like coil once inside the pore and maintain this coiled conformation until it escapes [36]. Over-

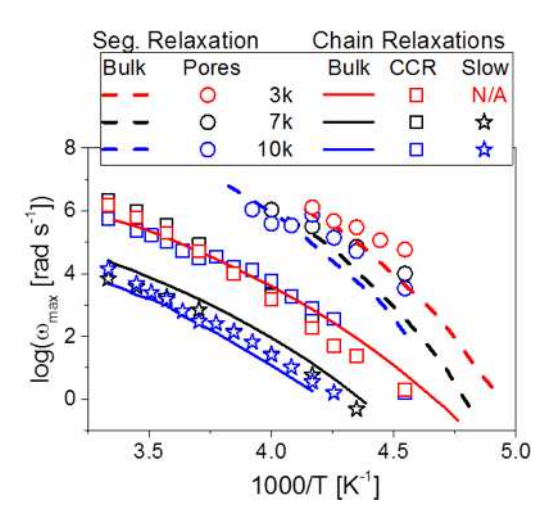


Fig. 4. The relaxation rates from all fits to dielectric spectra using eq. (1) for the 3 k (red), 7 k (black) and 10 k (blue) PI systems *versus* inverse temperature. Lines represent bulk relaxations of the polymer segments (dashed) and chains (solid). Symbols represent the segmental relaxation (circles), CCR (squares) and slow mode (stars).

all, these changes in the PI dielectric relaxations within 6.5 nm pores show that as the confinement becomes more extreme the dynamics of the polymer chain are significantly altered compared to previously reported systems that are confined at length-scales much larger than the polymer chain itself.

The average relaxation rates for the processes fit by eq. (1) are displayed against inverse temperature in fig. 4. The segmental relaxations of the confined systems have a weaker temperature dependence compared to bulk. This suggests a decrease in the relaxation time associated with the structural relaxation (i.e., a decrease in the dynamic glass transition temperature, T_g). This is consistent with changes in T_g for confined low molecular weight glass formers [15,20]. The rates for the segmental motions decrease with increasing molecular weight in both the bulk and under confinement. This increase in segmental relaxation times with molecular weight is consistent with the increase in T_g with molecular weight for unentangled systems as extensively discussed in the literature [37].

The mean chain relaxation rates for the bulk polymers slow down with increasing molecular weight in accordance with the predictions of the Rouse model for non-entangled chains [38]. The average CCR rates for confined 3 k PI in nanopores are very similar, but slightly slower compared to that observed in the bulk. As discussed before, this relaxation is significantly broadened under confinement. This relaxation rate also decreases faster with decreasing temperature compared to the bulk, and has a slightly more Arrhenius-like temperature dependence. This dependence is typically discussed in terms of lower fragility. However, the global fluctuations, such as the dynamics of the polymer chain, govern the rubbery plateau and viscoelastic flow. Therefore, this more Arrhenius-like temperature dependence can be considered in terms of less cooperativity of intra- and inter-chain motions allowing for increased

viscoelastic flow of the 3 k polymer under confinement, and is likely due to interactions with chains near the interface. This is consistent with two recent findings in the literature: 1) The diffusivity of confined polymers increases due to a decrease in the possible pathways (i.e. decreased tortuosity) of dynamical motion of polymer chains [39]; and 2) a lowered chain density under confinement due to interfacial adsorption [19]. Therefore, we speculate that there is higher free volume per chain and increased diffusivity of all of the PI M_w within nanopores. Furthermore, the similarity in the time-scales associated with the 3k chain in bulk and within pores suggests that the effects of surface interactions on dynamics is more influential than the geometric confinement itself at this degree of confinement. Here, we acknowledge recent reports on polymers confined within hard cylinders and in polymer thin films that show that equilibrium chain conformations are reached after very long annealing times [29, 30, 40, 41]. The dynamics described in these reports suggest that these equilibrium states after long times are not governed by changes in the time-scales relating to the dynamic glass transition, but are more closely related to time-scales associated with adsorption and desorption which are much slower than viscoelastic flow [10,29]. As significantly long times were reported for these equilibrium effects to take place (from a week and up to one month), this was beyond the primary goal of the present study. Additionally, by maintaining a constant pore size, we are assuming the surface area of the polymers in contact with the pore surface is held constant, while varying the molecular weight changes the relative number of segments contributing to the end-to-end chain relaxation causing the bimodal distribution of the chain relaxation into the CCR and slow relaxation in the 7k and 10k PI under confinement. However, we conjecture that, if given ample time, the structural/segmental PI relaxation rates may approach that of the bulk, but the chain relaxations will still be altered by the geometric confinement. We will now explore this point further by discussing the relaxation rates of the more confined, higher molecular weight PI.

The slowest relaxation, or "slow mode", observed for both $10\,\mathrm{k}$ and $7\,\mathrm{k}$ PI under confinement, but not in the $3\,\mathrm{k}$ PI, becomes more apparent as a low-frequency shoulder to the primary CCR relaxation with increasing molecular weight. The average rates of the slow mode for the 7 k PI are decreased compared to the normal mode of the bulk 7k PI. Slowed Rouse chain dynamics of confined polymers compared to bulk have been previously described through dynamical ¹H NMR and neutron scattering studies for pore sizes much greater than the dimensions of the chain [4,42,43]. At time-scales similar to that of the 7 k PI slow mode, the slow mode of the 10 k PI is observed. However, this relaxation is actually faster than its corresponding 10k chain relaxation in the bulk. The relative rates of the bulk chain relaxation divided by the slowest chain relaxation rates of all of our polymers in the pores is displayed in fig. 5. Here, we assume that the time-scales of the 3 k PI CCR are the slowest observed for this system. This ratio decreases with decreasing temperature for the 10 k PI, but increases slightly for the 3 k and 7 k PI. For

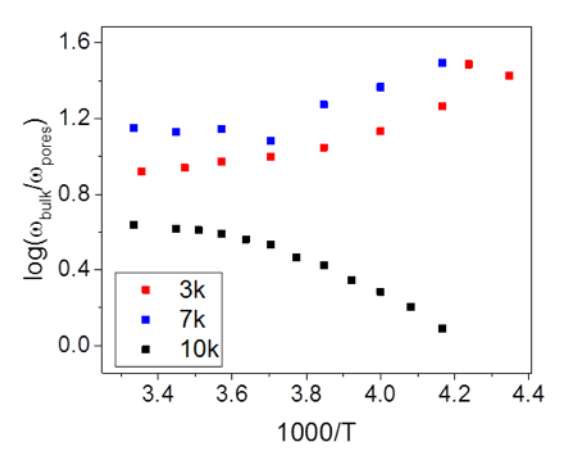


Fig. 5. The temperature dependence of the ratio between the bulk chain relaxation rate and the slowest relaxation rate observed for each polymer confined within 6.5 nm silica nanopores.

nanoconfined amino terminated and native PPG in native silica and silanized silica pores, respectively, this ratio is also observed to decrease with increasing confinement [19]. As such, we use a length-scale ratio of the pore diameter to the radius of gyration (D/R_q) of the bulk polymer to describe the degree of confinement. The R_q for our PI polymers was estimated from the hydrodynamic radius of PI in dioxane [44]. For the 3 k, 7 k, and 10 k PI systems, the respective D/R_g ratios are found to be 3.4, 2.3 and 1.9, respectively. For systems with large $D/R_q(>2.5)$ the resulting chain dynamics have been reported to have similar relaxation time-scales as observed in bulk [24]. As D/R_q decreases, the degree of confinement increases; thus, our results reveal that the time-scales associated with the polymer chain dynamics increase faster with temperature compared to the chain relaxation in bulk. We observe that at $D/R_q \sim 2$, the average slow chain relaxation rates become faster than that of the bulk. This was observed, but not highlighted or discussed in the recent report of PPG under confinement, and we compare these data in fig. S5 of the ESM [19]. The main result of the current article is that at extreme confinement length-scales, the relative rates of the chain dynamics under confinement begin to increase faster with temperature compared to bulk. Thus, we suggest that below $D/R_g \sim 2$ the degree of geometric confinement becomes an influential factor in the conformation of the polymer chains apart from just effects of interfacial interactions on segmental motion.

4 Conclusions

We have presented results from dielectric studies of low molecular weight poly(cis-1,4-isoprene) (PI) in bulk compared to identical systems in unidirectional silica nanopores with average diameter of 6.5 nm. The average size of the polymer chains as reflected by the radius of gyration (R_g) at these length-scales becomes comparable to that of the confining pore diameter. The only changes in the segmental dynamics observed under confinement are

the temperature dependence corresponding to the speeding up of the dynamic glass transition. However, a slow dielectric relaxation is observed with increasing molecular weight, while a primary chain relaxation occurs for all polymers at time-scales similar to that of the normal mode in bulk 3 k PI. The relative rates of the slow relaxation compared to bulk in the 7k and 10k PI under confinement are observed to change significantly. Additionally, the dielectric relaxation strengths of the less confined 3k and 7k PI are comparable in contrast to that of the confined 10 k PI. Furthermore, there is a decrease in the dielectric relaxation strength with decreasing temperature for the 10 k PI under confinement that we attribute to an increase in non-ideal chain conformations. Our primary observation is that a length-scale ratio of the pore diameter to the radius of gyration (D/R_g) at and below ~ 2 corresponds to a dramatic change in polymer dynamics due to the extreme confinement of the polymer chains forced to orient in non-ideal conformations. We propose that the geometric confinement of polymer chains at this length-scale ultimately becomes more influential on the chain dynamics compared to interfacial adsorption effects.

Financial support for contributions made by TK, EUM and JS were from the National Science Foundation (NSF), Division of Materials Research, Polymers Program through DMR-1905597. CI acknowledges the financial support of the project PN 19110204 by the Romanian Ministry of Scientific Research and Innovation.

Author contribution statement

Thomas Kinsey contributed the majority of the preparation and measurement of the materials, analysis of data and writing of this manuscript. Emmanuel Mapesa contributed greatly in editing and helpful discussion as an expert in confined polymer dynamics. Tyler Cosby began this original work as a graduate student, with guidance from Yangyang Wang, and graduated before the project was completed. The polymers were synthesized by Youjun He under supervision and guidance from Kunlun Hong. Ciprian Iacob originally prepared and developed the procedures for making the nanoporous silica membranes. Joshua Sangoro was the primary investigator contributing funding and direction for this research.

Publisher's Note The EPJ Publishers remain neutral with regard to jurisdictional claims in published maps and institutional affiliations.

References

- G.D. Smith, D.Y. Yoon, R.L. Jaffe, Macromolecules 25, 7011 (1992).
- K. Shin, S. Obukhov, J.T. Chen, J. Huh, Y. Hwang, S. Mok, P. Dobriyal, P. Thiyagarajan, T.P. Russell, Nat. Mater. 6, 961 (2007).

- D. Qi, Z. Fakhraai, J.A. Forrest, Phys. Rev. Lett. 101, 096101 (2008).
- M. Hofmann, A. Herrmann, S. Ok, C. Franz, D. Kruk, K. Saalwächter, M. Steinhart, E.A. Rössler, Macromolecules 44, 4017 (2011).
- M. Krutyeva, A. Wischnewski, M. Monkenbusch, L. Willner, J. Maiz, C. Mijangos, A. Arbe, J. Colmenero, A. Radulescu, O. Holderer, M. Ohl, D. Richter, Phys. Rev. Lett. 110, 108303 (2013).
- A. Schonhals, F. Rittig, J. Karger, J. Chem. Phys. 133, 094903 (2010).
- 7. S. Granick, Science **253**, 1374 (1991).
- C. Alba-Simionesco, B. Coasne, G. Dosseh, G. Dudziak, K.E. Gubbins, R. Radhakrishnan, M. Sliwinska-Bartkowiak, J. Phys.: Condens. Matter 18, R15 (2006).
- M. Alcoutlabi, G.B. McKenna, J. Phys.: Condens. Matter 17, R461 (2005).
- S. Napolitano, E. Glynos, N.B. Tito, Rep. Prog. Phys. 80, 036602 (2017).
- A. Serghei, D. Chen, D.H. Lee, T.P. Russell, Soft Matter 6, 1111 (2010).
- 12. A. Schönhals, R. Zorn, B. Frick, Polymer 105, 393 (2016).
- A. Schönhals, H. Goering, C. Schick, B. Frick, R. Zorn, Eur. Phys. J. E 12, 173 (2003).
- K. Adrjanowicz, R. Winkler, K. Chat, D.M. Duarte, W. Tu, A.B. Unni, M. Paluch, K.L. Ngai, Macromolecules 52, 3763 (2019).
- W.K. Kipnusu, M. Elsayed, R. Krause-Rehberg, F. Kremer, J. Chem. Phys. 146, 203302 (2017).
- M. Krutyeva, S. Pasini, M. Monkenbusch, J. Allgaier, J. Maiz, C. Mijangos, B. Hartmann-Azanza, M. Steinhart, N. Jalarvo, O. Ivanova, O. Holderer, A. Radulescu, M. Ohl, P. Falus, T. Unruh, D. Richter, J. Chem. Phys. 146, 203306 (2017).
- T. Uemura, N. Yanai, S. Watanabe, H. Tanaka, R. Numaguchi, M.T. Miyahara, Y. Ohta, M. Nagaoka, S. Kitagawa, Nat. Commun. 1, 83 (2010).
- M. Tarnacka, A. Talik, E. Kamińska, M. Geppert-Rybczyńska, K. Kaminski, M. Paluch, Macromolecules 52, 3516 (2019).
- W.K. Kipnusu, M.M. Elmahdy, M. Elsayed, R. Krause-Rehberg, F. Kremer, Macromolecules 52, 1864 (2019).
- 20. A. Schönhals, H. Goering, C. Schick, J. Non-Cryst. Solids **305**, 140 (2002).
- M. Tarnacka, K. Kaminski, E.U. Mapesa, E. Kaminska, M. Paluch, Macromolecules 49, 6678 (2016).
- J. Schueller, Y.B. Mel'nichenko, R. Richert, E.W. Fischer, Phys. Rev. Lett. 73, 2224 (1994).
- L. Petychakis, G. Floudas, G. Fleischer, Europhys. Lett. 40, 685 (1997).
- S. Alexandris, G. Sakellariou, M. Steinhart, G. Floudas, Macromolecules 47, 3895 (2014).
- E.U. Mapesa, L. Popp, W.K. Kipnusu, M. Tress, F. Kremer, Soft Mater. 12, S22 (2014).
- 26. W.H. Stockmeyer, Pure Appl. Chem. 15, 539 (1967).
- L. Zaraska, G.D. Sulka, M. Jaskuła, J. Solid State Electrochem. 15, 2427 (2011).
- D. Uhrig, J.W. Mays, J. Polym. Sci. Part A: Polym. Chem. 43, 6179 (2005).
- A. Panagopoulou, S. Napolitano, Phys. Rev. Lett. 119, 097801 (2017).
- 30. S. Napolitano, M. Wübbenhorst, Nat. Commun. 2, 260 (2011).

- F. Kremer, A. Schönhals, Broadband Dielectric Spectroscopy, 1 edition (Springer, Berlin, 2003) p. 729.
- W.H. Stockmeyer, M.E. Baur, J. Am. Chem. Soc. 86, 3485 (1964).
- C.M. Roland, M.J. Schroeder, J.J. Fontanella, K.L. Ngai, Macromolecules 37, 2630 (2004).
- 34. A. Serghei, F. Kremer, Phys. Rev. Lett. 91, 165702 (2003).
- Y. Yao, H.-J. Butt, J. Zhou, M. Doi, G. Floudas, Macro-molecules 51, 3059 (2018).
- L.Z. Sun, C.H. Wang, M.B. Luo, H. Li, J. Chem. Phys. 150, 024904 (2019).
- A. Elfadl, R. Kahlau, A. Herrmann, V.N. Novikov, E.A. Rössler, Macromolecules 43, 3340 (2010).
- 38. P.E. Rouse, J. Chem. Phys. 21, 1272 (1953).

- T. Zhang, K.I. Winey, R.A. Riggleman, Macromolecules
 22, 217 (2018).
- K. Adrjanowicz, M. Paluch, Phys. Rev. Lett. 122, 176101 (2019).
- C. Politidis, S. Alexandris, G. Sakellariou, M. Steinhart,
 G. Floudas, Macromolecules 52, 4185 (2019).
- M. Krutyeva, J. Martin, A. Arbe, J. Colmenero, C. Mijangos, G.J. Schneider, T. Unruh, Y. Su, D. Richter, J. Chem. Phys. 131, 174901 (2009).
- J. Martin, M. Krutyeva, M. Monkenbusch, A. Arbe, J. Allgaier, A. Radulescu, P. Falus, J. Maiz, C. Mijangos, J. Colmenero, D. Richter, Phys. Rev. Lett. 104, 197801 (2010).
- L.J. Fetters, N. Hadjichristidis, J.S. Lindner, J.W. Mays, J. Phys. Chem. Ref. Data 23, 619 (1994).